2010 3rd International Conference on Computer and Electrical Engineering (ICCEE 2010)
IPCSIT vol. 53 (2012) © (2012) IACSIT Press, Singapore
DOI: 10.7763/IPCSIT.2012.V53.No.1.12

SABER-Based Modeling and Simulation of Induction Motor Drive System for EVs

Ping Liu+, He-Ping Liu and Jun Guo

State Key Laboratory of Power Transmission Equipment & System Security and New Technology
Chongqing University, Chongqing, China

Abstract. Simulation tools are of great assistance to engineers and researchers to reduce product-development cycle time, improve the quality of the design, and simplify the analysis without costly and time-consuming experiments. In this paper, a model of Electric Vehicles (EVs) propulsion system has been constructed with the simulation platform SABER. It was chosen because of the robust modeling engine, the ease of integrating mechanical components, and the large library of existing models for a wide range of electrical components. This paper discusses the validity of the system model by creating module boxes for not only the electrical systems, but also the mechanical system of the vehicles. These modules include induction motors, voltage source inverters, vector control algorithm, and vehicle load torque module. The correctness and validity of this system are demonstrated by the simulation results of vector controlled induction motors and typical drive cycle condition. System-level analysis can be used to assess long-term behavior of EVs, and dynamic models are helpful to provide in-depth information about the short-term behavior of sublevel components. The model allows for real time evaluation of a wide range of parameters in vehicle operation as pure EVs.

Keywords: Electric Vehicles; induction motors; vector control; dynamic models; modeling and simulation

1. Introduction

At present, the crisis of energy shortage and the air pollution are the two obstacles that need to be solved urgently and it directly threatens the sustainable development of the traditional fuel vehicles. The development of electric vehicle technology has taken on an accelerated pace. Facing this situation, a large amount of money has been invested in automobiles by the global automotive manufacturer [1].

Electric propulsion system is the heart of EVs, and it directly determines the EVs performance [2]. The frequent and fast speed varying, acceleration and deceleration are desired in the traction motor. So the working characteristics of the traction motor that satisfy the driving behavior and dynamic behavior are the most ideal working characteristics, shown in Fig.1. The vector controlled inductor motor drive is most popular and mature. Its dynamic characteristics are very close to the ideal driving field of vehicle and its static characteristic, speed regulating range can satisfy the performance of electric propulsion system [3-4].

SABER is suitable for the electric automobiles hybrid system, because it is the unique multi-technology, multi-domain simulation software oriented to the mixture signal. It has become industry standard in many transnational corporations in the world especially in vehicle manufacturing field, such as

+ Corresponding author.
E-mail address: liuping@cqu.edu.cn.

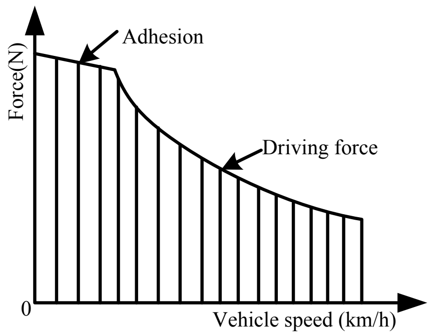

Figure 1. Ideal driving characteristics of vehicles

General Motors, Volkswagen, Chrysler Corporation. A large amount of money has been invested in SABER by these companies to satisfy the new need of engineering design.

SABER adapts the forward method to make simulation. Relations between components model will be more close to the actual situation of vehicle by using the forward method. The result of this method is more accurate than backward method in calculating the whole vehicle performance, but need more amount of computation. So the simulation time will be longer than the other simulation tools which use the backward method. In this paper, a drive system model for EVs is developed and analyzed. This component- and system-level analysis in automotive electrical and mechanical systems promises faster model creation and greater assurance of the analysis as compared with any step-by-step experimental work. As the SABER doesn't have every model we need, this paper adopts two methods to establish the basic framework, one is value assignment to the parameters which are provided by the software, the other is the MAST hardware description language available for accurately establish the behavioral models.

2. Implementation and Subsystem Models

Previously, EVs were mainly converted from the traditional fuel vehicles. The modern EVs are based on original body and frame designs to satisfy the structural requirements unique to EVs and to make use of the greater flexibility of electric propulsion. Fig.2 shows the system structure of EVs, consisting of motor controller, motor, reducer, battery, auxiliary subsystem and so on.

The simulation model of EVs drive system is built up according to the modern typical EV configuration, shown in Fig. 3.

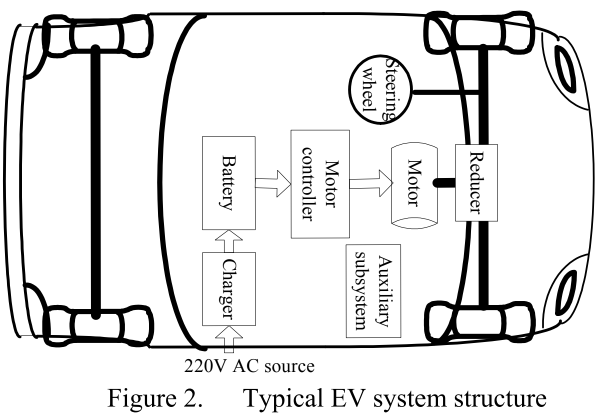

Figure 2. Typical EV system structure

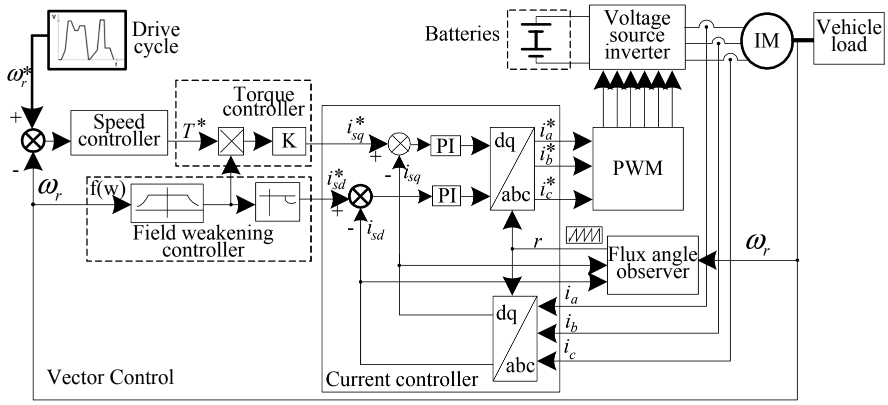

Figure 3. Block diagram of the control system for EVs

2.1 Induction motor

The induction motor drive has additional advantages such as lightweight nature, small volume, low cost, and high efficiency. These advantages are particularly important for EV applications. The model of the induction motor is synchronous frame by the key following equations [7-13]:

The voltage equation can be written in matrix format as

$$\begin{bmatrix} u_d \\ u_q \\ 0 \\ 0 \end{bmatrix} = \begin{bmatrix} R_s + L_s p & -\omega_s L_s & L_m p & -\omega_s L_m \\ \omega_s L_s & R_s + L_s p & \omega_s L_m & L_m p \\ L_m p & 0 & R_r + L_r p & 0 \\ \omega_{sl} L_m & 0 & \omega_{s1} L_r & R_r \end{bmatrix} \begin{bmatrix} i_{sd} \\ i_{sq} \\ i_{rd} \\ i_{rq} \end{bmatrix} \tag{1}$$

u_{sd}, u_{sq}, i_{sd} and i_{sq} are the dq-axis stator voltage and current components. i_{rd}, i_{rq} are the dq-axis rotor current components. R_s and R_r are the stator and rotor resistance respectively. L_s, L_r and L_m denote the stator, rotor self and mutual inductances respectively. $p = d/dt$, ω_s and ω_r denote the derivative operator, synchronous speed and rotor speed respectively. The slip speed is given as $\omega_{sl} = \omega_s - \omega_r$.

Then the flux linkage equation of an induction motor can be represented according to the usual dq components in a synchronous rotating frame as

$$\begin{bmatrix} \Psi_{sd} \\ \Psi_{sq} \\ \Psi_{rd} \\ 0 \end{bmatrix} = \begin{bmatrix} L_s & 0 & L_m & 0 \\ 0 & L_s & 0 & L_m \\ L_m & 0 & L_r & 0 \\ 0 & L_m & 0 & L_r \end{bmatrix} \begin{bmatrix} i_{sd} \\ i_{sq} \\ i_{rd} \\ i_{rq} \end{bmatrix} \tag{2}$$

Ψ_{sd} Ψ_{sq} and Ψ_{rd} are the dq-axis stator flux linkage and the d-axis rotor flux linkage.

The rotor flux linkage equation can be derived from equation (2):

$$\Psi_r = \frac{L_m}{1 + T_r p} i_{sd} \tag{3}$$

where the $T_r = L_r / R_r$ is rotor time constant.

The torque is expressed in terms of the stator current and rotor flux, can be derived as follows

$$T_e = p \frac{L_m}{L_r} \Psi_r i_{sq} \tag{4}$$

where T_e is electromagnetic torque, p is the number of pole pairs.

2.2 Vector control strategy

Vector control can realize the optimal control for transient operation of an induction motor drive. Both the magnetic field and the torque developed in the motor can be controlled independently. The vector control strategy block is comprised of speed controller, torque controller, field weakening controller, current controller, rotor flux angle observer and voltage source inverter. Each of these sub-systems is described below.

1) speed controller

The block diagram of speed controller is shown in Fig.4. The motor rotational speed is compared with the reference speed to generate the speed error signal w_diff . It t is then fed through the speed controller to get the commanded torque signal T_q_max . The speed controller used in the example is a classical PI controller.

1) Field weakening controller

This paper adopts the simple field weakening method that is

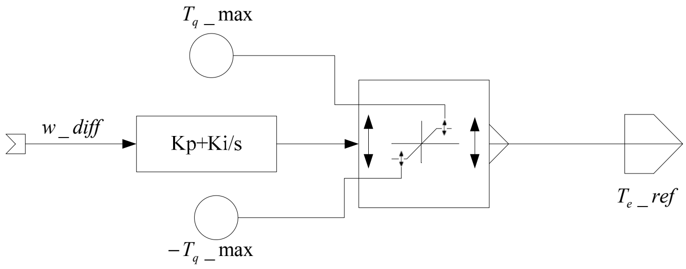

Figure 4. Block diagram of speed controller

to vary the stator field reference in portion to $1/\omega_r$. The d-axis current i_{sd}^* is expressed in terms of a speed function and the base field current i_{sdbase} under base speed.

$$i_{sd}^* = f(\omega) i_{sdbase} \tag{5}$$

The speed function with the following characteristics is applied:

$$\begin{aligned} f(\omega) &= \frac{\omega_b}{\omega_r}; \qquad |\omega_b| < |\omega_r| < |\omega_{\max}| \\ &= 1; \qquad 0 \le |\omega_r| \le |\omega_b| \end{aligned} \tag{6}$$

The output of the speed function is unity up to the base speed and decreases hyperbolically with speed between the base and the maximum speed to ensure constant output power.

2) torque controller

Torque equation (4) can be rewritten as

$$\begin{aligned} T_e &= p\frac{L_m^2}{L_r(1+T_r \bullet p)} i_{sd} i_{sq} \\ &= p\frac{L_m^2}{L_r(1+T_r \bullet p)} i_{sdbase} f(\omega) i_{sq} \end{aligned} \tag{7}$$

Setting the $K_T = p\frac{L_m^2}{L_r(1+T_r \bullet p)} i_{sdbase}$, we can obtain:

$$i_{sq}^* = T_{qcmd} f(\omega) \frac{1}{K_T} \tag{8}$$

Block diagram of torque controller is shown in Fig. 5.

3) rotor flux angle observer and current controller

The theory of the flux angle estimation is derived from the following equations.

$$\theta_{\psi r} = \int \omega_{\psi r} dt \tag{9}$$

$$\omega_{\psi r} = \omega_r + \omega_{sl} \tag{10}$$

$$\omega_{sl} = \frac{1}{T_r}\frac{i_{sq}^*}{i_{sd}^*} \tag{11}$$

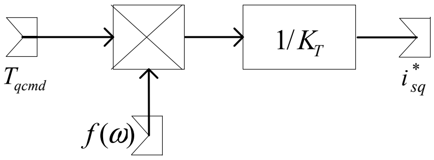

Figure 5. Block diagram of torque controller

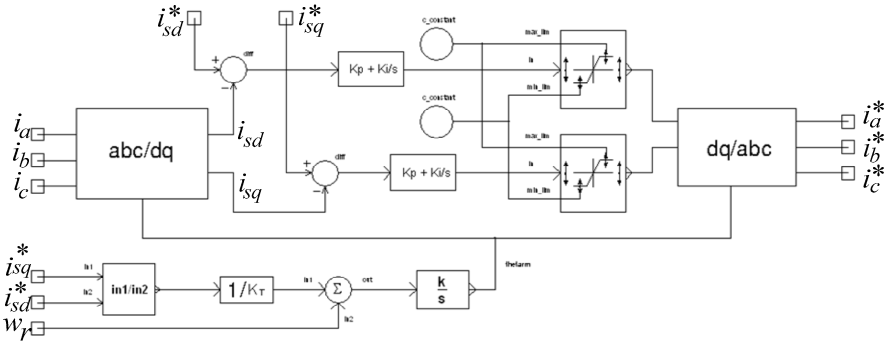

Figure 6. Block diagram of current controller

In (11), $T_r = L_r / R_r$, the influence of mutual inductance L_m is neglected. Although the calculation about ω_{sl} is approximate estimation and it is not accuracy at the dynamic variation process, it is less influenced by the harmonic current.

The block diagram of current controller is shown in Fig. 6. The dq-axis rotor currents (i_{sd}, i_{sq}) are obtained from the phase currents (i_a, i_b and i_c), compared with the reference currents (i_{sd}^*, i_{sq}^*) to generate the error signals. The error signals are then converted back to abc-axis as i_a^*, i_b^* and i_c^* through the proportional integral (PI) controllers, used to compared with the triangular wave in the PWM module for generating the gating signal to drive the switches in the inverter.

2.3 Vehicle load module

The load of the motor is a reducer connected to a simplified vehicle dynamic model. Referring to the vehicle dynamics theory, the total resistance force consists of rolling resistance F_f, aerodynamic resistance F_W, and gravitational force F_i and acceleration resistance F_j.

Hence, the vehicle load dynamic equation can be obtained as:

$$\sum F = F_w + F_f + F_i + F_j \tag{12}$$

$$\begin{cases} F_w = C_d \rho A v^2 \\ F_f = fmgcos\alpha \\ F_i = mgsin\alpha \\ F_j = \delta mdv/dt \end{cases} \tag{13}$$

where A is the frontal area(m2), C_d is the aerodynamic resistance coefficient, ρ is the air density(kg/m3), v is the vehicle speed(km/h), f is the rolling resistance coefficient, α is the road angle(rad), δ is the conversion coefficient of vehicle mass (δ>l), m is the vehicle mass(kg), dv/dt is the vehicle acceleration(m/s^2). The aerodynamic resistance coefficient and rolling resistance are existence on the level ground, but the grade resistance and acceleration resistance can be found with special driving conditions. The both ends of equation (12) can be multiplied with the vehicle speed, and the mechanical

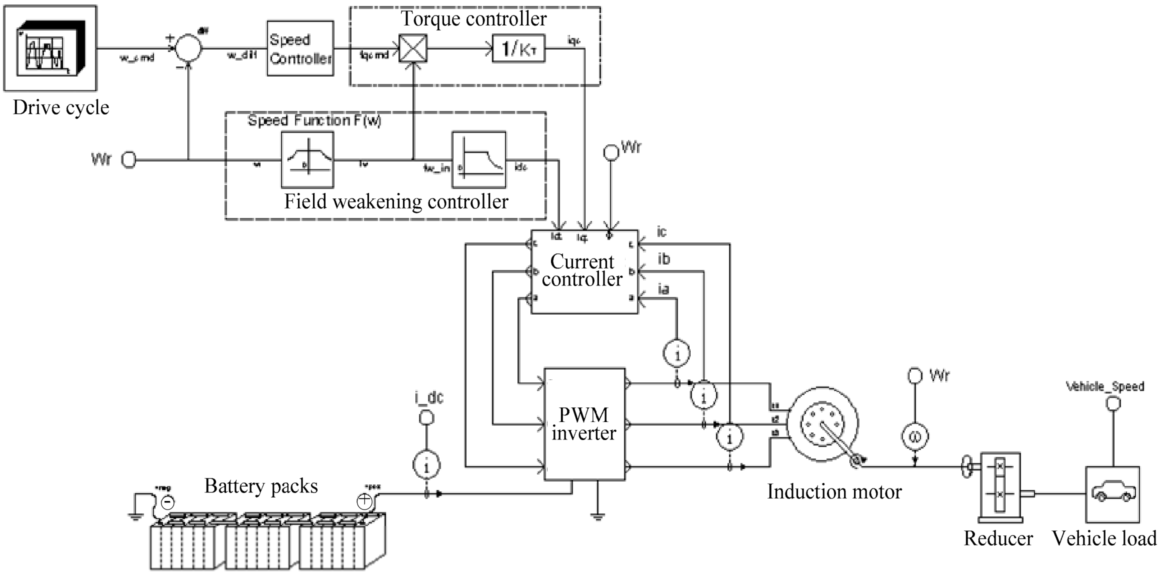

Figure 7. Block diagram of EVs propulsion system simulation model

losses are considered, then output power of motor can be obtained:

$$P_M = \frac{1}{\eta}\left(\frac{mgfv\cos\alpha}{3600} + \frac{mgv\sin\alpha}{3600} + \frac{C_d A v^3}{76140} + \frac{\delta m v}{3600} \bullet \frac{dv}{dt}\right) \tag{14}$$

where P_M is the output power of motor.

2.4 System model

The simulation model of vector controlled induction motor propulsion system for EVs is shown in Fig. 7.

3. Simulation analysis

Table I gives the information about EVs specifications.

Table 1. EV model specifications

Components	Parameter	Value
Induction motor	Rated power	5 kW
	Maximum power	15 kW
	Rated speed	3000 r/min
	Maximum speed	6000 r/min
	Rated torque	15.8 N • m
	Maximum torque	62 N • m
Battery	Rated voltage	48 V
	Rated capacity	200 A • h
Transmission system	Reduction ratio	7
	Power train efficiency	0.9
Vehicle parameters	Gross mass	860 kg
	Frontal area	1.7 m^2
	Rolling Resistance Coefficient	0.015
	Radius of wheels	0.266 m
	Aerodynamic drag Coefficient	0.3

3.1 Transient analysis simulation of vector control

Fig. 8 shows the simulation results of output power, output torque of induction motor, the reference and real motor speed. The test presented here is in different operation points. First the vehicle starts and it drives at a reference speed equal to 3000 rpm which is the rated motor speed. Next, the vehicle drives at 6000 rpm which is the maximum motor. Finally the vehicle is stopped. It shows the real motor speed following the reference speed. We can also conclude that the flux and torque controls are well decoupled. A very good static and dynamic behavior of the system is noted.

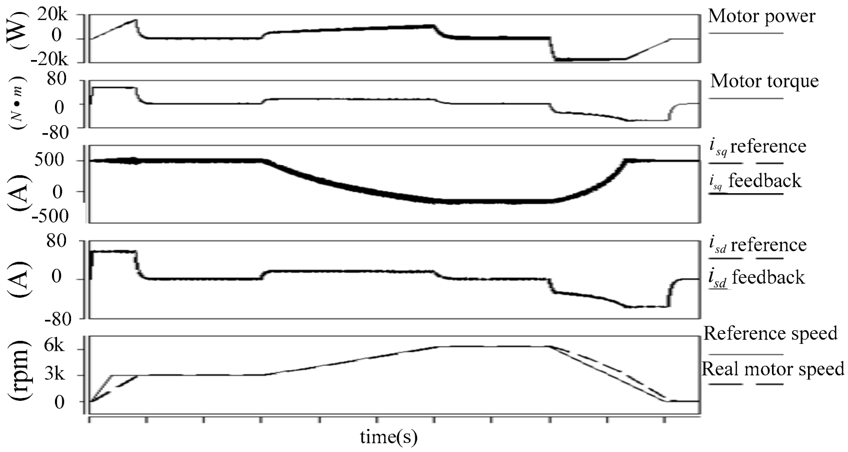

Figure 8. Motor dynamic response on the level ground

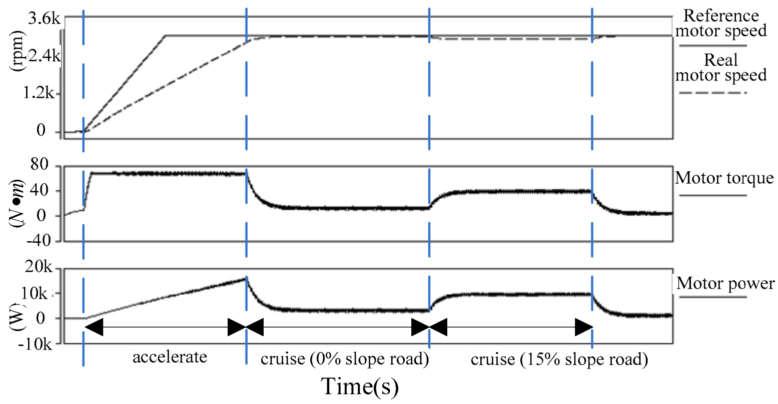

Figure 9. Motor dynamic response in different operation state

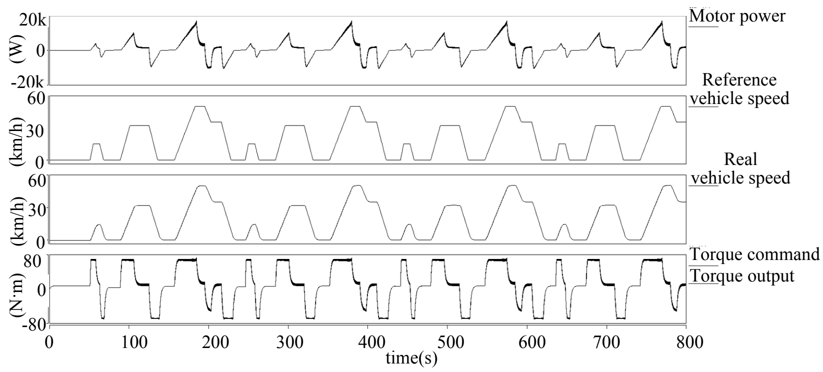

Figure 10. Simulations results of drive cycle ECE-15

The dynamic response results in different operation state, illustrated in the Fig. 9 can be divided in four state: the first state is a acceleration process, the second one is a cruise process with 0% slope road, the third one is a cruise process with 15% slope road and the last one is the same to the second.

From the Fig. 8 and Fig. 9 we could know:

(1) As mentioned before, the load torque depends on travel total resistances, which include rolling resistance, aerodynamic resistance, gravitational force and acceleration resistance. The maximum torque of the traction motor is generated at the acceleration process of the vehicle. And the peak power is generated at the end of the accelerate process.

(2) When the vehicle cruises with 0% slope road, the motor output torque and power just need to overcome the constant moving resistance. So the output torque and power both are a smaller constant value.

(3) When the vehicle is climbing with 15% slope road, the total resistances include the gravitational resistance. So when selecting the peak power and maximum torque of the traction motor it is determined by the maximum resistance taking into accounts the maximum slope road.

3.2 Drive cycle simulation

Fig. 10 is the simulation result of the output power, reference vehicle speed, real vehicle speed, torque command and feedback torque during an ECE-15 drive cycle. This driving cycle represents urban driving. It is characterized by low vehicle speed (max.50 km/h) and is useful for testing small EVs performance. The obtained results seem to be very promising. We can see that vehicle speed and torque can rapidly following the reference value at this cycle mode.

4. Conclusions

Because the electric-propulsion system is the key component of EVs dynamic system, the performance of propulsion system impacts the overall performance of EVs directly. There are a number of the designing and analysis of vehicle with steady-state modeling simulation in recent years. SABER has been able to show the capabilities of simulating not only the electrical systems, but also the mechanical and other systems of a vehicle.

In this paper, we have presented a modeling tool that has the advantages of utilizing capabilities of the SABER software in detailed. And the model of EVs propulsion system is constructed by the dynamic model of subsystems, and the simulation verified vector control strategy of motor and EVs propulsion system which has better dynamic and static characteristics. The design scheme and parameters can be flexibly adjusted and optimized properly by simulation analysis, which can predict the performance of EVs and its subsystem. It shows the Saber simulator is well suited to design and verify the motor drive system used in electric/hybrid vehicles.

5. References

[1] Chan C C. The State of the Art of Electric, Hybrid and Fuel Cell Vehicles[J]. Proceedings of the IEEE, 2007,95(4):704-718.

[2] C C Chan, K T Chau. Modern EVs technology[M]. Oxford University Press, USA, 2001.

[3] Zeraoulia M, Benbouzid M E H, Diallo D. Electric motor drive selection issues for HEV propulsion systems:A Comparative Study[J]. IEEE Transactions on Vehicular Technology, 2006, 55(6): 1756-1764.

[4] HE HONG-WEN, YU XIAO-JIANG, SUN FENG-CHUN. Study on power performance of traction motor system for EVs[J]. Proceedings of the CSEE, 2006, 26(6):136-140.

[5] AMRHEIN M, KREIN P T. Dynamic simulation for analysis of hybrid EVs system and subsystem interactions, including power electronics[J]. Vehicular Technology, IEEE Transactions on, 2005, 54(3): 825-836

[6] ZHANG XIANG, QIAN LI-JUN, ZHANG BING-LI, et al. State-of-the-art of EVs simulation software [J]. Journal of System Simulation, 2004, 16(8):1621-1623.

[7] M Ehsani, Y Gao, S Gay, A. Emadi. Modern Electric, Hybrid Electric, and Fuel Cell Vehicles: Fundamentals, Theory, and Design [M]. CRC Press, 2004.

[8] CUI PEI-LIANG, ZHAO KE-YOU. Modeling and simulation of induction motor vector control based on MALAB/simulink S-Function [J]. Journal of System Simulation, 2005, 17(z2):86-90.

[9] ZHOU SONG-LIN, ZHU YUN-GUO, GONG ZHAO-TIAN. Simulation experiment platform of AC asynchronism motor vector control system based on SABER[J]. Coal Mine Machinery, 2007,28(12): 49-52.

[10] WANG YI, MA HONG-FEI, ZHAO KAI-QI, et al. Field-oriented vector control of induction motor for EVs[J]. Proceedings of the CSEE, 2005, 25(11): 113-117.

[11] Liu Yan, Shao Cheng, Ding Yuan-ming. Modeling and simulating of variable parameters induction motors in EVs applications[J]. Journal of System Simulation, 2006, 18(12): 3358-3361.

[12] Chen Yong, Zhang Da-ming, Jiang Pi-jie. Simulation analysis of vector control system for asynchronous motor in EVs[J]. Journal of System Simulation, 2007, 19(16): 3761-3765.

[13] Vasudevan M, Arumugam R, Paramasivam S. Modelling and simulation of a hybrid vehicle using direct torque control of induction motor[J]. International Journal of Modelling and Simulation,2007,27(1):80-88.

[14] Huijuan liu, Yihuang zhang, Qionglin zheng. Design and simulation of an inverter-fed induction motor for EVs[C]. 2007 Vehicle Power and Propulsion Conference, September 9-12, 2007, Arlington, TX, USA: IEEE, 2008:4

[15] Manigrasso R, Mapelli F.L. Design and modeling of asynchronous traction drives fed by limited power source[C]//2005 IEEE Vehicle Power and Propulsion Conference, September 7-9, 2005, Chicago, IL, USA: IEEE,2006:36-43

[16] Fernando Briz,Alberto Diez,Michael W Degner,etal. Current and Flux Regulation in Field-Weakening Operation[J].IEEE Trans.on Indus. Appl. 2001, 37(1):42-51.

[17] XU HONG-GUO. Automobile theory[M]. China Communications Press